

## Strain-Based Echocardiographic Evaluation of Myocardial Adaptation in Normal Pregnancy: Insights into Physiological Remodeling

### Strain-Tabanlı Ekokardiyografik Değerlendirme: Normal Gebelikte Miyokardiyal Adaptasyon ve Fizyolojik Yeniden Yapılanmaya İlişkin Bulgular

#### ABSTRACT

**Objective:** The aim of this study was to investigate longitudinal changes in biventricular diastolic function and myocardial deformation during pregnancy and the early postpartum period using tissue Doppler imaging (TDI), speckle-tracking echocardiography (STE), and rotational mechanics.

**Method:** In this prospective observational study, 65 healthy, normotensive women with singleton pregnancies underwent echocardiography at four standardized time points: first trimester (10–12 weeks), second trimester (20–24 weeks), third trimester (36–38 weeks), and early postpartum (6–12 weeks post-delivery). Comprehensive evaluation included conventional Doppler, TDI-derived parameters, longitudinal strain rates, atrial strain, and left ventricular (LV) twist mechanics.

**Results:** Pregnancy was characterized by a progressive rise in cardiac output and ventricular volumes, with parallel declines in diastolic indices and atrial function. Although LV ejection fraction remained preserved, early diastolic strain rate decreased by 19% ( $1.59 \rightarrow 1.29 \text{ s}^{-1}$ ,  $P < 0.001$ ), lateral Em velocity declined by 20%, and global LV twist was reduced by 20% ( $17.8^\circ \rightarrow 14.2^\circ$ ,  $P = 0.002$ ). The mitral E/A ratio progressively decreased, while deceleration time remained prolonged postpartum ( $203 \rightarrow 243 \text{ ms}$ ,  $P < 0.001$ ). Atrial strain analysis revealed chamber-specific remodeling: left atrial conduit strain showed near recovery, whereas right atrial parameters showed only partial normalization. Collectively, these findings indicate that diastolic and torsional mechanics did not fully normalize within 6–12 weeks, suggesting heterogeneous recovery trajectories even among healthy pregnancies.

**Conclusion:** In healthy women, pregnancy-induced myocardial adaptation appears to involve progressive diastolic and deformation changes that may persist into the early postpartum phase. The observation of residual subclinical alterations—despite otherwise physiological remodeling—suggests that longitudinal surveillance could be valuable, even in low-risk populations. Advanced echocardiographic modalities may improve early detection and contribute to refined risk stratification in pregnancy-related cardiac adaptation.

**Keywords:** Diastolic function, left ventricular twist, myocardial adaptation, postpartum recovery, pregnancy, speckle-tracking echocardiography, strain rate

#### ÖZET

**Amaç:** Gebelik ve erken postpartum dönemde biventriküler diyastolik fonksiyon ile miyokardiyal deformasyon değişikliklerini doku Doppler görüntüleme (TDI), speckle-tracking ekokardiyografi (STE) ve rotasyonel mekanikler kullanarak değerlendirmek.

**Yöntem:** Bu prospektif gözlemsel çalışmaya, tekil gebeliği olan 65 sağlıklı ve normotansif kadın dahil edildi. Ekokardiyografik incelemeler dört standart zaman noktasında gerçekleştirildi: birinci trimester (10–12 hafta), ikinci trimester (20–24 hafta), üçüncü trimester (36–38 hafta) ve erken postpartum dönem (doğumdan 6–12 hafta sonra). Kapsamlı değerlendirme; konvansiyonel Doppler, TDI parametreleri, longitudinal strain hızları, atriyal strain ve sol ventrikül (LV) twist mekaniklerini içermektedir.

**Bulgular:** Gebelik süresince kardiyak debi ve ventrikül hacimleri kademeli olarak artarken, diyastolik indeksler ve atriyal fonksiyonlarda belirgin düşüşler izlendi. LV ejeksiyon fraksiyonu korunmuş olmasına rağmen erken diyastolik strain hızı %19 azaldı ( $1.59 \rightarrow 1.29 \text{ s}^{-1}$ ,  $P < 0.001$ ), lateral Em hızı %20 düştü ve global LV twist %20 azaldı ( $17.8^\circ \rightarrow 14.2^\circ$ ,  $P = 0.002$ ). Mitral E/A oranı kademeli olarak azalırken, deselerasyon zamanı postpartum dönemde de uzamış kaldı

#### ORIGINAL ARTICLE KLİNİK ÇALIŞMA

Seda Tanyeri Uzel<sup>1</sup>

Barkin Kültürsay<sup>2</sup>

Murat Karaçam<sup>3</sup>

Rezzan Deniz Acar<sup>1</sup>

Berhan Keskin<sup>4</sup>

Ali Karagöz<sup>1</sup>

<sup>1</sup>Department of Cardiology, Kartal Koşuyolu Training and Research Hospital, Istanbul, Türkiye

<sup>2</sup>Department of Cardiology, Tunceli State Hospital, Tunceli, Türkiye

<sup>3</sup>Department of Cardiology, Bitlis State Hospital, Bitlis, Türkiye

<sup>4</sup>Department of Cardiology, Bağcılar Medipol Mega University Hospital, Istanbul, Türkiye

**Corresponding author:**

Seda Tanyeri Uzel

✉ sedatanyeri@hotmail.com

**Received:** October 08, 2025

**Accepted:** December 15, 2025

**Cite this article as:** Tanyeri Uzel S, Kültürsay B, Karaçam M, Acar RD, Keskin B, Karagöz A. Strain-Based Echocardiographic Evaluation of Myocardial Adaptation in Normal Pregnancy: Insights into Physiological Remodeling. *Türk Kardiyol Dern Ars.* 2026;54(2):152–164.

DOI: 10.5543/tkda.2025.89335



Copyright@Author(s)

Available online at [archivestsc.com](http://archivestsc.com).

Content of this journal is licensed under a Creative Commons Attribution – NonCommercial–NoDerivatives 4.0 International License.

(203→243 ms,  $P < 0.001$ ). Atriyal strain analizinde odacığa özgü farklılıklar görüldü: sol atriyal conduit strain postpartum normale yakın seyrederken, sağ atriyal parametrelerde toparlanma belirgin olarak daha yavaş seyretti. Bu bulgular, diyastolik ve torsiyonel mekaniklerin 6–12 hafta içinde tamamen düzelmediğini ve sağlıklı gebeliklerde bile toparlanma sürecinin heterojen seyrettiğini göstermektedir.

**Sonuç:** Sağlıklı kadınlarda gebeliğe bağlı miyokardiyal adaptasyon, erken postpartum dönemde de sürebilen progresif diyastolik ve deformasyon değişikliklerini içermektedir. Fizyolojik yeniden yapılanmaya rağmen gözlenen subklinik değişiklikler, düşük riskli popülasyonlarda bile kardiyak fonksiyonların uzunlamasına takibinin değerli olabileceğini düşündürmektedir. İleri ekokardiyografik yöntemler, erken tanıya katkı sağlayabilir ve gebelikle ilişkili kardiyak adaptasyonda daha hassas risk sınıflamasına destek olabilir.

**Anahtar Kelimeler:** Diyastolik fonksiyon, sol ventrikül bükülmesi, miyokardiyal adaptasyon, postpartum iyileşme, gebelik, speckle-tracking ekokardiyografi, strain hızı

Pregnancy imposes one of the most profound physiological demands on the maternal cardiovascular system. To meet the metabolic needs of the developing fetus, cardiac output increases by 30–50%, plasma volume expands, heart rate rises, and systemic vascular resistance decreases markedly.<sup>1–3</sup> While these adaptations are considered physiological, the sustained hemodynamic load creates a unique environment in which subtle alterations in cardiac structure and function may occur. Increasing evidence suggests that such changes may extend into the postpartum period and potentially influence long-term cardiovascular health in women.<sup>4–7</sup>

The left ventricular (LV) diastolic function is particularly sensitive to fluctuations in preload and afterload. Prior studies have reported decreases in the E/A ratio, reductions in Em velocity, and prolongation of deceleration time during pregnancy.<sup>8</sup> However, these data are largely derived from cross-sectional designs, limiting the ability to characterize the dynamic trajectory of diastolic adaptation across pregnancy.<sup>9</sup> Moreover, the degree to which these alterations normalize postpartum remains incompletely defined, as systematic early postpartum evaluations are scarce.<sup>10</sup>

Conventional echocardiographic parameters provide important but limited insight into the complex interplay between systolic, diastolic, and torsional mechanics during pregnancy. Advanced echocardiographic modalities, such as speckle-tracking, strain rate imaging, and rotational mechanics, offer higher temporal resolution and greater sensitivity to subclinical myocardial changes, making them particularly valuable in physiological states characterized by rapidly shifting loading conditions.<sup>11–13</sup> Strain rate, in particular, is less preload-dependent than conventional strain and may better reflect intrinsic myocardial relaxation properties during gestation. Despite these advantages, few longitudinal studies have integrated deformation imaging, rotational mechanics, and atrial strain in the same cohort. Additionally, atrial adaptation—a key component of ventricular filling—remains underinvestigated, especially with respect to chamber-specific remodeling patterns. Given that atrial function is highly dependent on LV relaxation and chamber compliance, a comprehensive assessment of both atria may provide additional insight into normal gestational remodeling.

## ABBREVIATIONS

Ap CSR-E	Apical circumferential early diastolic strain rate
Ap RR-E	Apical early diastolic rotational rate
Ap RSR-E	Apical radial early diastolic strain rate
ASE	American Society of Echocardiography
AVC	Aortic valve closure
BMI	Body mass index
EACVI	European Association of Cardiovascular Imaging
ECG	Electrocardiography
ESC	European Society of Cardiology
GLS	Global longitudinal strain
ICC	Intraclass correlation coefficient
IVRT	Isovolumic relaxation time
IVV	Isovolumic myocardial velocity
LA SR-E	Left atrial early diastolic strain rate
LSR-E	Early diastolic longitudinal strain rate
LVEDD	Left ventricular end-diastolic diameter
LVEDV	Left ventricular end-diastolic volume
LVEF	Left ventricular ejection fraction
MAPSE	Mitral annular plane systolic excursion
STE	Speckle-tracking echocardiography
TAPSE	Tricuspid annular plane systolic excursion
TDI	Tissue Doppler imaging

To address these gaps, we designed a prospective, longitudinal study incorporating conventional Doppler indices, tissue Doppler imaging, strain rate parameters, and rotational mechanics to characterize physiological cardiac adaptation across pregnancy and into the early postpartum period. This integrated approach allows for a detailed evaluation of ventricular relaxation, deformation, atrial mechanics, and torsional behavior, providing a more complete understanding of maternal myocardial remodeling.

Importantly, the 2025 European Society of Cardiology (ESC) Guidelines identify pregnancy as a natural "cardiovascular stress test" that can unmask latent susceptibility to future cardiovascular disease and emphasize the importance of postpartum surveillance.<sup>3</sup> In this context, our study aims to clarify the temporal evolution of myocardial mechanical changes during pregnancy and to determine the degree of functional recovery within the early postpartum window, thereby contributing contemporary, guideline-aligned evidence to the growing field of pregnancy-related cardiac physiology.

## Materials and Methods

### Study Design and Population

This prospective, single-center study evaluated trimester-specific and postpartum cardiac changes using advanced echocardiographic modalities. Sixty-nine healthy women with uncomplicated singleton pregnancies were consecutively enrolled between January 2022 and August 2023 at a tertiary academic hospital. Four participants were excluded due to chronic hypertension. The final cohort consisted of 65 normotensive women with no prior cardiovascular, renal, pulmonary, or metabolic disease.

To ensure data consistency, only term pregnancies ( $\geq 37$  weeks of gestation) were eligible for the final analysis; women who experienced preterm delivery were excluded by design. Additional exclusion criteria included gestational hypertension, preeclampsia, gestational diabetes, multiple gestation, fetal anomalies or growth restriction, structural heart disease, arrhythmia, and use of cardioactive medications.<sup>5</sup> All participants provided written informed consent, and the study was approved by Kartal Koşuyolu High Specialization Training and Research Hospital Scientific Research Ethics Committee (Approval Number: 2025/12/1196, Date: 22.07.2025) in accordance with the Declaration of Helsinki.

Echocardiographic evaluations were performed at four predefined time points: first trimester (10–12 weeks), second trimester (20–24 weeks), third trimester (36–38 weeks), and early postpartum (6–12 weeks after delivery). For each participant, gestational age at delivery and mode of delivery (vaginal vs. cesarean section) were prospectively recorded. Maternal age, body mass index (BMI), gestational weight gain, and maternal weight change postpartum were recorded at each visit.

### Imaging Strategy and Rationale

To account for the dynamic hemodynamic changes of pregnancy, we focused on deformation-based measurements with higher temporal sensitivity. Strain-rate imaging was preferred because it is less preload-dependent and better reflects trimester-specific changes in myocardial relaxation. Rotational mechanics (basal and apical rotation and LV twist) were added to assess torsional adaptation, while bilateral atrial strain-rate analysis provided chamber-specific information on reservoir, conduit, and contractile function. Overall, this multimodal approach enabled a comprehensive and physiologically sensitive evaluation of cardiac remodeling during pregnancy and the early postpartum period.

### Echocardiographic Acquisition and Analysis

All echocardiographic examinations were performed using a standardized protocol with a Vivid 7 ultrasound system (GE Vingmed, Norway) equipped with a 2.5-MHz phased-array transducer. Images were acquired with participants in the left lateral decubitus position, during quiet respiration, and with simultaneous electrocardiographic (ECG) gating. Harmonic imaging was used in all studies. A single experienced sonographer performed all acquisitions to minimize inter-operator variability. Offline analyses were conducted using EchoPAC PC software (GE Healthcare). All measurements were averaged over three consecutive cardiac cycles.

Left ventricular volumes were calculated using Simpson's biplane method, and left ventricular ejection fraction (LVEF) was derived accordingly. Longitudinal systolic function was assessed via mitral annular plane systolic excursion (MAPSE) and tricuspid annular plane systolic excursion (TAPSE).<sup>14</sup> Due to the focus on functional assessment, we did not evaluate left ventricular mass, right ventricular dimensions, pulmonary pressures, or indexed atrial volumes in this study. The left atrial area was used as a surrogate for atrial remodeling.

Pulsed-wave Doppler was used to measure mitral and tricuspid inflow velocities (E, A, E/A ratio, and deceleration time). The Doppler sample volume (2–3 mm) was placed at the leaflet tips with an insonation angle  $< 15^\circ$  whenever possible. Tissue Doppler imaging (TDI) was performed at a sweep speed of 100 mm/s. Early (Em) and late (Am) diastolic myocardial velocities were obtained from the septal and lateral mitral annulus using a 3–5 mm sample volume. Isovolumic relaxation time (IVRT) was measured using continuous-wave Doppler with cursor alignment toward the LV outflow tract–mitral inflow junction. Isovolumic myocardial velocity (IVV) was obtained from TDI traces during the isovolumic relaxation period.<sup>15</sup>

Although global longitudinal strain (GLS) is a widely used deformation parameter, we intentionally focused on strain-rate-based measurements in this study. Strain rate provides higher temporal resolution and is less influenced by preload fluctuations, which is particularly relevant in pregnancy, where loading conditions vary substantially across trimesters. To maintain methodological consistency and enhance sensitivity to dynamic hemodynamic changes, GLS was not included in the primary analysis set.

Longitudinal strain rate was measured from apical four-, two-, and three-chamber views using speckle-tracking echocardiography. Frame rates were maintained between 60 and 90 frames per second, meeting American Society of Echocardiography (ASE)/European Association of Cardiovascular Imaging (EACVI) recommendations, and frame-rate optimization ensured a temporal resolution-to-heart-rate ratio  $> 0.7$ . Segments with suboptimal tracking were manually adjusted; persistent tracking failure resulted in segment exclusion and reacquisition when feasible. In line with guideline standards, analyses were accepted only when  $\geq 12$  of 16 left ventricular segments demonstrated adequate tracking quality. Key parameters included early diastolic longitudinal strain rate (LSR-E), late diastolic longitudinal strain rate (LSR-A), and systolic longitudinal strain rate (LSR-S). Atrial strain rates were obtained by tracing the atrial endocardial border, referencing end-diastole as the zero-strain point. Early and late diastolic atrial strain rates were calculated from the respective filling phases.<sup>11,12,16</sup>

In addition to strain-rate parameters, left atrial reservoir strain was also measured from apical four-chamber views using speckle-tracking echocardiography, and its temporal changes were evaluated as part of a supplementary analysis.

LV rotational mechanics were assessed from parasternal short-axis views at the basal level (mitral valve) and apical level (just distal to the papillary muscles). Tracking was performed ensuring clear visualization of endocardial and epicardial borders. Global

LV twist was calculated as the instantaneous difference between apical and basal rotation. Rotational rate curves were derived from the first derivative of rotational displacement, and systolic (RR-S), early diastolic (RR-E), and late diastolic (RR-A) rotational rates were quantified. Aortic valve closure (AVC) was identified using Doppler or TDI to mark end-systole.

### Statistical Analysis

Data distribution was assessed using the Kolmogorov-Smirnov test. Continuous variables were expressed as mean  $\pm$  standard deviation or median with interquartile range. Repeated-measures Analysis of Variance (ANOVA) or Friedman tests were used for longitudinal comparisons, with Bonferroni-corrected post hoc analyses for pairwise comparisons. Given the homogeneity of the study cohort, multivariable modeling and correlation analyses with clinical covariates were not performed.

Sample size was calculated based on an expected 15% change in Em velocity (standard deviation [SD] 2.5 cm/s), with 80% power and  $\alpha = 0.05$ , yielding a requirement of 45 participants. To allow for attrition, 65 were enrolled. Complete data were available for all participants.

Intra-observer reproducibility was assessed in 20 randomly selected cases (five per time point). The same observer repeated all measurements two weeks later using the same software. Intraclass correlation coefficients (ICCs) indicated excellent reliability:  $> 0.90$  for Doppler measures,  $> 0.85$  for strain rate,  $> 0.82$  for rotational mechanics, and  $> 0.80$  for atrial strain.

A  $p$ -value  $< 0.05$  was considered statistically significant. All analyses were performed using SPSS version 26 (IBM Corp., NY, USA).

## Results

### Baseline Characteristics

Of the 69 women initially recruited, four were excluded due to a history of chronic hypertension. The final cohort comprised 65 healthy, normotensive pregnant women, with a mean age of  $28.6 \pm 5.4$  years and a baseline BMI of  $25.6 \pm 4.1$  kg/m<sup>2</sup>. All pregnancies resulted in term deliveries ( $\geq 37$  weeks), as preterm births were excluded by study design. The mean gestational age at delivery was  $38.6 \pm 1.1$  weeks, and the mode of delivery included vaginal birth in 60% and cesarean section in 40% of participants. Maternal weight increased from  $66 \pm 9$  kg in the first trimester to  $75 \pm 10$  kg in the third trimester and decreased to  $69 \pm 9$  kg postpartum ( $P < 0.001$ ) (Table 1).

Systolic and diastolic blood pressures remained stable during early pregnancy, increased in the third trimester (systolic:  $102 \pm 11$  to  $113 \pm 11$  mmHg; diastolic:  $65 \pm 8$  to  $69 \pm 6$  mmHg), and decreased postpartum ( $110 \pm 10$  and  $67 \pm 5$  mmHg, respectively). Mean arterial pressure followed a similar pattern ( $78 \pm 7 \rightarrow 80 \pm 10 \rightarrow 75 \pm 8$  mmHg;  $P < 0.001$ ). Heart rate increased progressively during gestation from  $72 \pm 11$  bpm in the first trimester, peaked at  $81 \pm 11$  bpm in the third trimester, and declined to  $75 \pm 8$  bpm after delivery, remaining slightly higher than first-trimester values ( $P < 0.001$ ) (Table 1).

### Changes in Left Ventricular Structure and Systolic Function

Left ventricular end-diastolic diameter (LVEDD) and end-diastolic volume (LVEDV) increased across pregnancy, peaked in

the third trimester, and decreased postpartum. LVEDD increased from  $4.58 \pm 0.39$  cm to  $4.72 \pm 0.40$  cm in the third trimester, then decreased to  $4.40 \pm 0.38$  cm postpartum ( $P < 0.001$ ). LVEDV rose from  $79.3 \pm 16.9$  mL to  $126 \pm 22.1$  mL (59% increase) and declined to  $98.9 \pm 23.9$  mL postpartum. Left ventricular end-systolic volume (LVESV) increased from  $34.9 \pm 9.52$  mL to  $53.8 \pm 12.6$  mL and decreased to  $46.3 \pm 10.2$  mL postpartum ( $P < 0.001$ ) (Table 1).

Left ventricular ejection fraction (LVEF) was  $65.5 \pm 6.3\%$  in the first trimester and  $61.5 \pm 7.4\%$  postpartum ( $P = 0.009$ ). TAPSE and MAPSE values decreased in the third trimester and increased postpartum (TAPSE:  $2.32 \pm 0.32 \rightarrow 2.31 \pm 0.41 \rightarrow 2.55 \pm 0.28$  cm; MAPSE:  $1.46 \pm 0.22 \rightarrow 1.40 \pm 0.27 \rightarrow 1.53 \pm 0.14$  cm) (Table 1).

### Left Ventricular Diastolic Function

Mitral early diastolic inflow velocity (E wave) decreased from  $0.86 \pm 0.16$  m/s in the first trimester to  $0.60 \pm 0.14$  m/s postpartum ( $P < 0.001$ ). A-wave velocity showed a similar pattern, declining from  $0.65 \pm 0.15$  m/s to  $0.50 \pm 0.16$  m/s ( $P < 0.001$ ). Accordingly, the E/A ratio progressively decreased throughout pregnancy. Deceleration time (DT) increased from  $203 \pm 41.2$  ms in the first trimester to  $273 \pm 27.6$  ms in the third trimester and remained prolonged postpartum ( $243 \pm 15.6$  ms;  $P < 0.001$ ). Left atrial area also increased significantly—from  $10.5 \pm 2.29$  cm<sup>2</sup> in the first trimester to  $15.5 \pm 2.67$  cm<sup>2</sup> in the third trimester—and, although it partially regressed postpartum, it remained elevated at  $14.6 \pm 2.23$  cm<sup>2</sup> ( $P < 0.001$ ) (Figure 1).

Lateral Em velocity declined from  $-0.173 \pm 0.03$  cm/s to  $-0.138 \pm 0.02$  cm/s ( $P < 0.001$ ) and remained reduced postpartum. Septal Em and Am velocities also decreased significantly across pregnancy (Em:  $-0.118 \pm 0.03 \rightarrow -0.094 \pm 0.02$  cm/s; Am:  $-0.104 \pm 0.03 \rightarrow -0.078 \pm 0.01$  cm/s; both  $P < 0.001$ ). Lateral Sm similarly decreased from  $0.114 \pm 0.02$  cm/s to  $0.106 \pm 0.02$  cm/s postpartum ( $P = 0.001$ ) (Table 1, Figure 2). Lateral, septal, and averaged E/Em ratios progressively increased throughout pregnancy, reflecting physiologic augmentation of filling pressures, and showed partial improvement during the early postpartum period (Table 1).

Septal IVV increased from  $2.54 \pm 1.16$  ms to  $4.12 \pm 1.20$  ms in the third trimester ( $P < 0.001$ ), whereas lateral IVV remained elevated postpartum ( $4.20 \pm 2.35 \rightarrow 4.15 \pm 0.94$  ms;  $P = 0.033$ ). Septal IVRT rose from  $38.2 \pm 9.54$  ms in the first trimester to  $42.6 \pm 9.13$  ms in the third trimester and decreased to  $35.9 \pm 7.22$  ms postpartum ( $P < 0.001$ ). Lateral IVRT showed a similar trend, increasing to  $40.4 \pm 9.96$  ms in late pregnancy and regressing to  $35.9 \pm 7.11$  ms postpartum, although this change did not reach statistical significance ( $P = 0.067$ ) (Figure 3).

### Right Ventricular Diastolic Function

Right ventricular diastolic indices showed clear trimester-related changes that only partially normalized postpartum. Tricuspid inflow velocities progressively declined throughout pregnancy; the E wave decreased from  $0.63 \pm 0.15$  m/s to  $0.42 \pm 0.04$  m/s and the A wave from  $0.54 \pm 0.13$  m/s to  $0.42 \pm 0.08$  m/s (both  $P < 0.001$ ). In parallel, tricuspid deceleration time lengthened markedly in late pregnancy ( $200 \pm 69.8$  ms  $\rightarrow$   $268 \pm 29.5$  ms) and remained prolonged after delivery ( $263 \pm 20.1$  ms;  $P < 0.001$ ).

**Table 1. Clinical characteristics and echocardiographic structural, systolic, and diastolic parameters across pregnancy and postpartum**

Clinical characteristics	1 <sup>st</sup> trimester	2 <sup>nd</sup> trimester	3 <sup>rd</sup> trimester	Postpartum	P
Cardiac chamber dimensions and systolic function parameters					
Weight (kg)	66 ± 9	69 ± 10	75 ± 10	69 ± 9	<0.001 <sup>a,b,c,d,f</sup>
Systolic BP (mm Hg)	102 ± 11	100 ± 12	113 ± 11	110 ± 10	<0.001 <sup>b,c,d,e</sup>
Diastolic BP (mm Hg)	65 ± 8	63 ± 7	69 ± 6	67 ± 5	<0.001 <sup>b,d,e</sup>
Mean BP (mm Hg)	78 ± 7	74 ± 5	80 ± 10	75 ± 8	<0.001 <sup>a,d,f</sup>
Heart rate (bpm)	72 ± 11	80 ± 10	81 ± 11	75 ± 8	<0.001 <sup>a,b,c,e,f</sup>
Structural and systolic function parameters					
LV EDD (cm)	4.58 ± 0.39	4.74 ± 0.36	4.72 ± 0.40	4.40 ± 0.38	<0.001 <sup>c,e,f</sup>
LV ESD (cm)	2.90 ± 0.36	2.97 ± 0.35	3.01 ± 0.40	2.93 ± 0.32	0.335
LV EDV (mL)	79.3 ± 16.9	108 ± 21.6	126 ± 22.1	98.9 ± 23.9	<0.001 <sup>a,b,c,d,e,f</sup>
LV ESV (mL)	34.9 ± 9.52	47.5 ± 12.7	53.8 ± 12.6	46.3 ± 10.2	<0.001 <sup>a,b,c,d,f</sup>
EF (%)	65.5 ± 6.29	65.5 ± 10.0	64.4 ± 7.17	61.5 ± 7.42	0.009 <sup>c,e</sup>
TAPSE (cm)	2.32 ± 0.32	2.45 ± 0.29	2.31 ± 0.41	2.55 ± 0.28	<0.001 <sup>c,f</sup>
MAPSE (cm)	1.46 ± 0.22	1.40 ± 0.22	1.40 ± 0.27	1.53 ± 0.14	0.002 <sup>e,f</sup>
LA area (cm <sup>2</sup> )	10.5 ± 2.29	13.0 ± 2.27	15.5 ± 2.67	14.6 ± 2.23	<0.001 <sup>a,b,c,d,e,f</sup>
Left ventricular (LV) diastolic function parameters					
E (m/s)	0.86 ± 0.16	0.79 ± 0.17	0.65 ± 0.14	0.60 ± 0.14	<0.001 <sup>b,c,d,e</sup>
A (m/s)	0.65 ± 0.15	0.63 ± 0.13	0.64 ± 0.16	0.50 ± 0.16	<0.001 <sup>c,e,f</sup>
DT (ms)	203 ± 41.2	250 ± 41.9	273 ± 27.6	243 ± 15.6	<0.001 <sup>a,b,c,d,e,f</sup>
Lat Em (cm/s)	-0.173 ± 0.03	-0.157 ± 0.03	-0.138 ± 0.04	-0.138 ± 0.02	<0.001 <sup>b,c,d,e</sup>
Sep Em (cm/s)	-0.118 ± 0.03	-0.106 ± 0.02	-0.086 ± 0.02	-0.094 ± 0.02	<0.001 <sup>b,c,d</sup>
Lateral E/Em	5.20 ± 1.34	5.26 ± 1.52	5.12 ± 2.01	4.49 ± 1.33	
Septal E/Em	7.78 ± 2.18	7.83 ± 2.22	8.08 ± 2.65	6.65 ± 1.59	
Averaged E/Em	6.49 ± 1.52	6.54 ± 1.76	6.60 ± 1.88	5.57 ± 1.29	

BP, Blood pressure; EF, Ejection fraction; LA area, Left atrial area; LV EDD, Left ventricular end-diastolic diameter; LV EDV, Left ventricular end-diastolic volume; LV ESD, Left ventricular end-systolic diameter; LV ESV, Left ventricular end-systolic volume; MAPSE, Mitral annular plane systolic excursion; mean BP, Mean arterial pressure; TAPSE, Tricuspid annular plane systolic excursion; A, Late diastolic mitral inflow velocity; averaged E/Em, Mean of lateral and septal E/Em ratios; DT, Mitral E-wave deceleration time; E, Early diastolic mitral inflow velocity; lat Em, Lateral early diastolic myocardial velocity (tissue Doppler imaging); lat E/Em, Ratio of mitral E velocity to lateral Em myocardial velocity; sep Em, Septal early diastolic myocardial velocity (tissue Doppler imaging); sep E/Em, Ratio of mitral E velocity to septal Em myocardial velocity. a, First trimester vs. second trimester; b, First trimester vs. third trimester; c, First trimester vs. postpartum; d, Second trimester vs. third trimester; e, Second trimester vs. postpartum; f, Third trimester vs. postpartum.

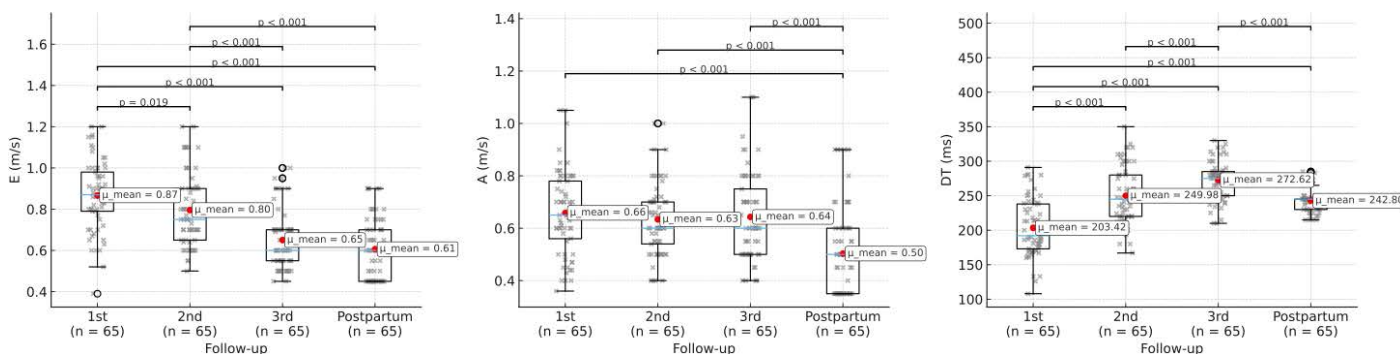


**Figure 1. Longitudinal changes in E-wave, A-wave, and deceleration time (DT) across pregnancy and postpartum. Box plots illustrate temporal variations in E-wave velocity (left), A-wave velocity (middle), and deceleration time (right) measured during the first, second, and third trimesters, as well as postpartum.**

Tissue Doppler findings were consistent with impaired relaxation. Right ventricular (RV) Em velocity decreased significantly to  $-0.123 \pm 0.02$  cm/s postpartum ( $P < 0.001$ ), and RV Am velocity similarly declined ( $-0.118 \pm 0.03$  cm/s;  $P < 0.001$ ). RV Sm initially rose slightly in mid-pregnancy but fell below baseline in the postpartum period ( $P < 0.001$ ).

Isovolumic parameters also varied across pregnancy. Lateral IVRT increased from  $60.8 \pm 10.2$  ms to  $63.1 \pm 8.07$  ms in the third trimester and decreased to  $57.3 \pm 6.3$  ms postpartum ( $P = 0.001$ ). Lateral IVV increased from  $8.07 \pm 3.01$  ms to  $11.0 \pm 2.52$  ms in late pregnancy and partially decreased to  $9.08 \pm 1.92$  ms postpartum ( $P < 0.001$ ) (Figures 4, 5).

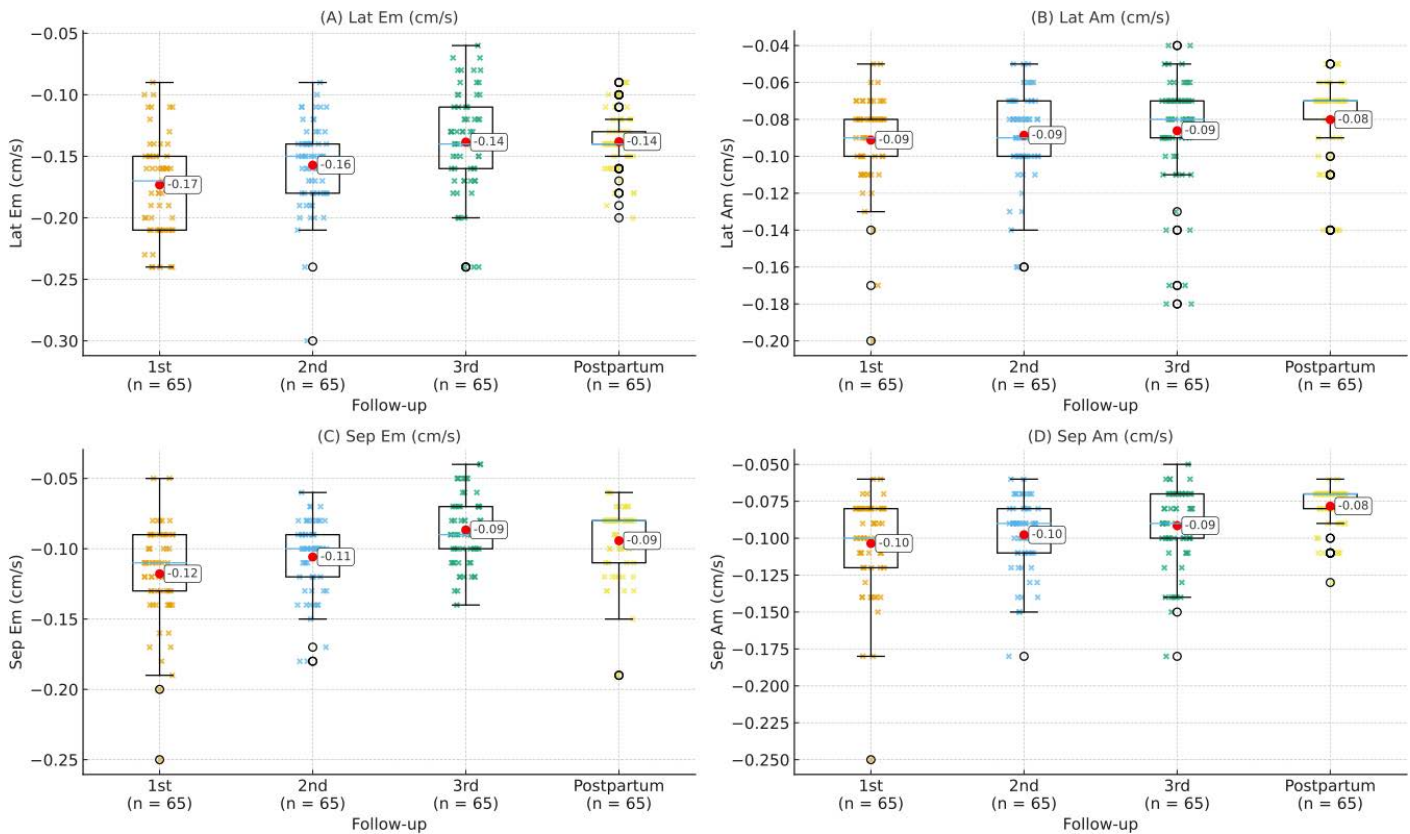


**Figure 2. Longitudinal changes in tissue Doppler imaging-derived (TDI-derived) diastolic parameters across pregnancy and postpartum. Temporal changes in TDI-derived lateral and septal early diastolic velocity (Em) and atrial contraction velocity (Am) are shown. A significant decline in Em is observed throughout pregnancy and remains reduced postpartum despite normalized preload ( $P < 0.001$ ). Am also progressively decreases, particularly in the septal segment ( $P < 0.001$ ).**

## Strain Rate Parameters and Rotational Mechanics

### Left Ventricular Strain Rate Analysis

Left ventricular early diastolic strain rate declined across all apical views. LSR-E decreased from  $1.59$  to  $1.29$   $s^{-1}$  in the four-chamber view, from  $1.57$  to  $1.36$   $s^{-1}$  in the two-chamber view, and from  $1.61$  to  $1.09$   $s^{-1}$  in the three-chamber view (all  $P < 0.001$ ). Similarly, apical circumferential early diastolic strain rate (Ap CSR-E) decreased from  $2.56$  to  $1.91$   $s^{-1}$  ( $P < 0.001$ ), whereas apical radial early diastolic strain rate (Ap RSR-E) remained stable throughout pregnancy ( $P = 0.587$ ) (Table 3, Figure 6). Other basal and apical strain-rate components (e.g., Basal SR-S, Basal RSR-E, Ap CSR-A) showed smaller trimester-related variations without a uniform pattern, and their detailed values are presented in Table 3.

### Rotational Mechanics

Left ventricular rotational parameters showed distinct trimester-related changes (Table 2).

Basal rotation remained stable across pregnancy and postpartum ( $-5.51^\circ \rightarrow -5.04^\circ$ ,  $P = 0.800$ ), whereas apical rotation decreased from  $12.4^\circ$  in the first trimester to  $9.16^\circ$  postpartum ( $P = 0.002$ ). Global LV twist declined from  $17.8^\circ$  to  $14.2^\circ$  in the postpartum period ( $P = 0.002$ ). The LV systolic rotational rate (LV RR-S) decreased from  $120^\circ/s$  to  $97.2^\circ/s$  ( $P = 0.005$ ), and early diastolic rotational rate (LV RR-E) declined from  $-119^\circ/s$  to  $-95.5^\circ/s$  ( $P = 0.027$ ). Late diastolic rotational rate (LV RR-A) did not show a significant overall change ( $P = 0.173$ ).

Basal systolic rotational rate (Baz RR-S) decreased from  $-71.3^\circ/s$  to  $-49.7^\circ/s$  ( $P < 0.001$ ), while basal late diastolic rotational rate (Baz RR-A) increased from  $42.5^\circ/s$  to  $54.3^\circ/s$  ( $P = 0.001$ ). Basal early diastolic rotational rate remained unchanged (Baz RR-E:  $60.4^\circ/s \rightarrow 58^\circ/s$ ,  $P = 0.307$ ). Apical early diastolic rotational rate (Ap RR-E) showed a significant change across pregnancy and postpartum ( $-90.9^\circ/s \rightarrow -80.5^\circ/s$ ,  $P = 0.022$ ), whereas apical systolic and late diastolic rotational rates (Ap RR-S and Ap RR-A) did not demonstrate significant overall variation (both  $P > 0.05$ ).

### Atrial Strain-Rate Analysis

Left atrial early diastolic strain rate (LA SR-E) declined from  $-2.26 \pm 0.65$   $s^{-1}$  in the first trimester to  $-1.85 \pm 0.51$   $s^{-1}$  in the second trimester but recovered to  $-2.25 \pm 0.65$   $s^{-1}$  postpartum ( $P < 0.001$ ). Late diastolic values (LA SR-A) showed a modest temporal fluctuation across pregnancy ( $P = 0.020$ ). Consistent with these changes, LA reservoir strain also varied significantly over time (Appendix Table 1).

Right atrial (RA) strain-rate values demonstrated a similar trimester-related pattern. Early diastolic strain rate (RA SR-E) decreased during pregnancy ( $-1.92 \pm 0.75 \rightarrow -2.13 \pm 1.05$   $s^{-1}$ ) and partially improved postpartum ( $-1.42 \pm 0.77$   $s^{-1}$ ;  $P < 0.001$ ). Late diastolic RA SR-A showed a mild reduction postpartum compared with baseline ( $-1.62 \pm 0.61 \rightarrow -1.36 \pm 0.54$   $s^{-1}$ ;  $P = 0.04$ ). In contrast, systolic strain rate (RA SR-S) progressively increased throughout pregnancy and into the postpartum period ( $1.85 \pm 0.53 \rightarrow 2.19 \pm 0.48$   $s^{-1}$ ;  $P < 0.001$ ).

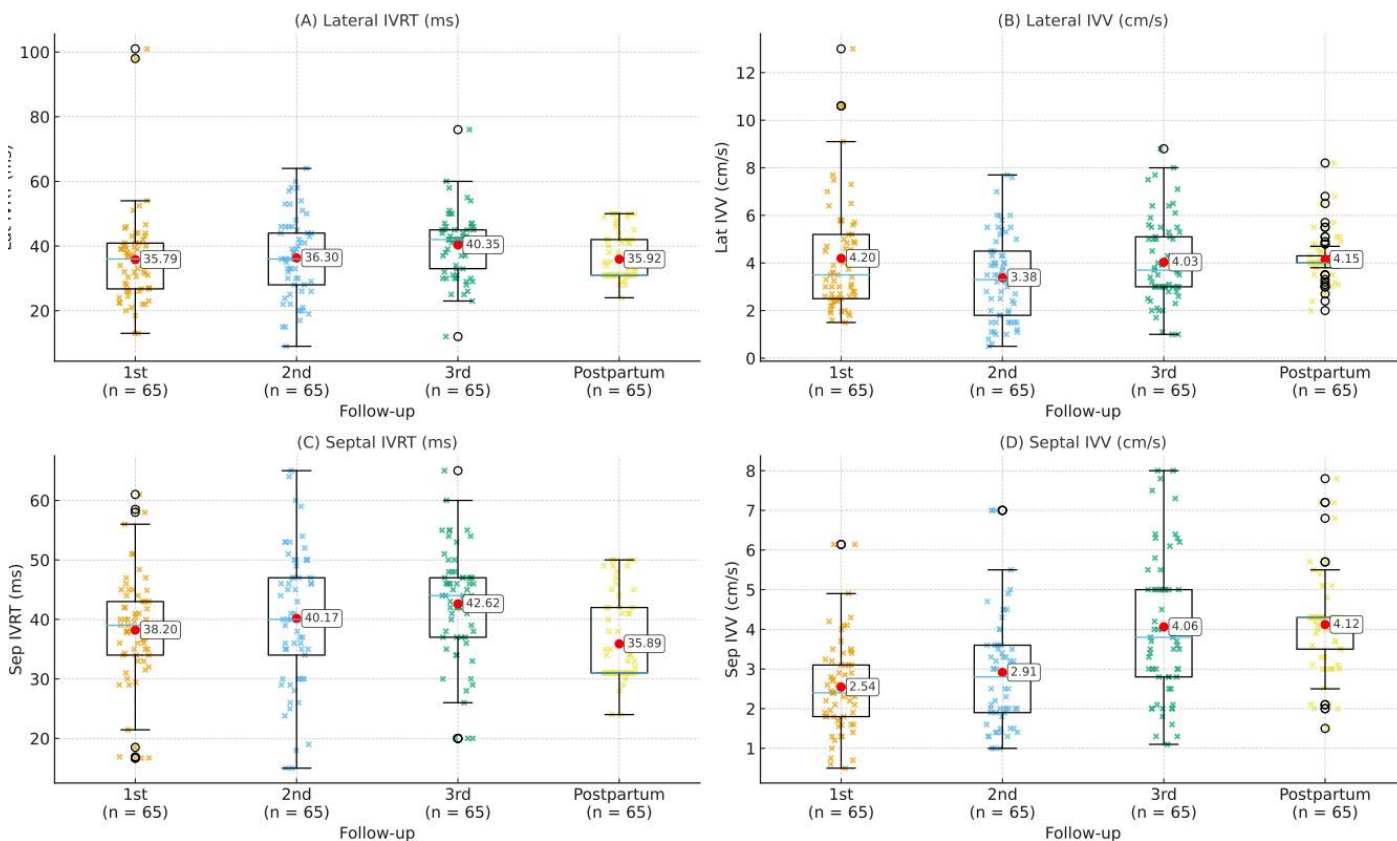


**Figure 3. Longitudinal changes in isovolumetric relaxation parameters across pregnancy and postpartum. This figure illustrates changes in isovolumetric velocity (IVV) and isovolumetric relaxation time (IVRT) in the lateral and septal segments during pregnancy and postpartum.**

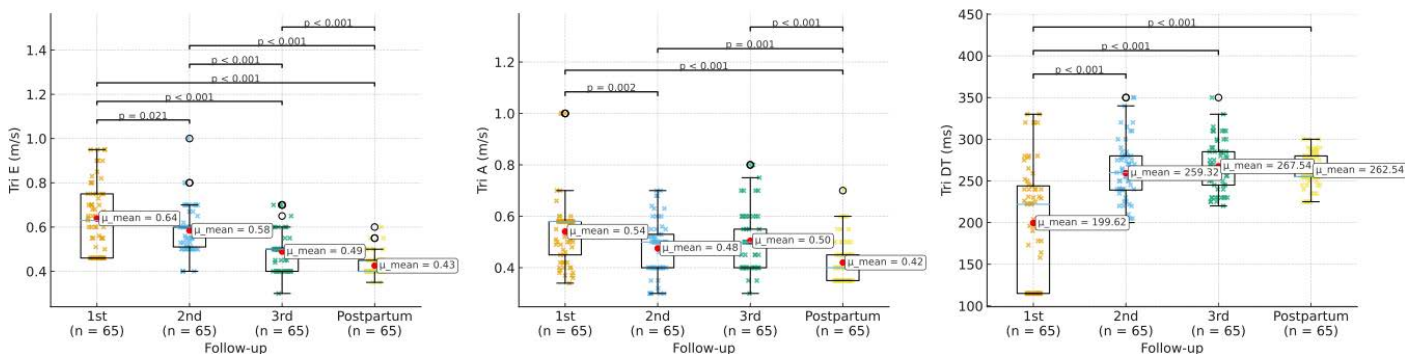


**Figure 4. Longitudinal changes in tricuspid inflow parameters across pregnancy and postpartum. Temporal variations in tricuspid inflow (Tri) parameters—early diastolic velocity (Tri E), late diastolic velocity (Tri A), and deceleration time (Tri DT)—are depicted across pregnancy and postpartum.**

These chamber-specific patterns are illustrated in Figure 7 (biatrial strain-rate curves) and detailed in Table 3 and Appendix Table 1.

**Discussion**

This prospective longitudinal study offers one of the most detailed evaluations to date of physiological cardiac adaptation during healthy pregnancy by integrating conventional Doppler, tissue Doppler imaging, strain-rate analysis, and rotational mechanics across gestation and into the early postpartum period. Unlike prior investigations that relied predominantly on cross-sectional

assessments or focused primarily on LV systolic indices,<sup>9,17</sup> our multimodal approach enabled a chamber-specific and temporally resolved characterization of both ventricular and atrial function.

Across pregnancy, we observed progressive trimester-related alterations in several diastolic markers—including reductions in early diastolic tissue Doppler velocities (Em), early diastolic longitudinal strain rate (LSR-E), and dynamic changes in atrial strain-rate parameters—suggesting physiologic modulation of myocardial relaxation. Although LV ejection fraction remained within normal limits, a small but statistically significant decline was detected,

**Table 2. Changes in rotational mechanics parameters during pregnancy and the postpartum period**

Parameter	1 <sup>st</sup> trimester	2 <sup>nd</sup> trimester	3 <sup>rd</sup> trimester	Postpartum	P
Rotational mechanics parameters					
Baz Rot (°)	-5.51 ± 2.77	-5.35 ± 2.50	-5.42 ± 3.15	-5.04 ± 2.90	0.800
Ap Rot (°)	12.4 ± 6.42	9.54 ± 4.96	11.1 ± 4.80	9.16 ± 4.55	0.002 <sup>a,c</sup>
LV twist (°)	17.8 ± 6.99	14.9 ± 5.39	16.5 ± 5.88	14.2 ± 4.96	0.002 <sup>a,c</sup>
LV RR S (°/s)	120 ± 42.5	112 ± 44	123 ± 50.4	97.2 ± 40.2	0.005 <sup>c,f</sup>
LV RR E (°/s)	-119 ± 53.5	-99.9 ± 42.3	-106 ± 52.2	-95.5 ± 38.1	0.027 <sup>c</sup>
LV RR A (°/s)	-83.4 ± 46.9	-68.1 ± 36.9	-79.6 ± 54	-71.5 ± 35.6	0.173
Baz RR S (°/s)	-71.3 ± 28.1	-63.6 ± 28.6	-61.7 ± 28.9	-49.7 ± 26.8	<0.001 <sup>c,e</sup>
Baz RR E (°/s)	60.4 ± 31.7	51.9 ± 46	58.7 ± 27.5	58 ± 24.1	0.307
Baz RR A (°/s)	42.5 ± 22.6	37.3 ± 17.6	44.9 ± 28.9	54.3 ± 27.2	0.001 <sup>c,e</sup>
Ap RR S (°/s)	79.3 ± 35.9	77.6 ± 39	87 ± 43.3	75.8 ± 25.5	0.317
Ap RR E (°/s)	-90.9 ± 53.7	-70.9 ± 37.1	-70.7 ± 43.3	-80.5 ± 43.2	0.022 <sup>b</sup>
Ap RR A (°/s)	-68.3 ± 36.9	-56.1 ± 30.6	-69.8 ± 39	-56.4 ± 43.5	0.058

Ap RR S/E/A, Apical rotational rate during systole, early diastole, and late diastole; Baz/Ap Rot, Basal and apical rotation angle; Baz RR S/E/A, Basal rotational rate during systole, early diastole, and late diastole; LV RR S/E/A, Left ventricular rotational rate during systole, early diastole, and late diastole; LV Twist, Left ventricular twist. a, First trimester vs. second trimester; b, First trimester vs. third trimester; c, First trimester vs. postpartum; d, Second trimester vs. third trimester; e, Second trimester vs. postpartum; f, Third trimester vs. postpartum.

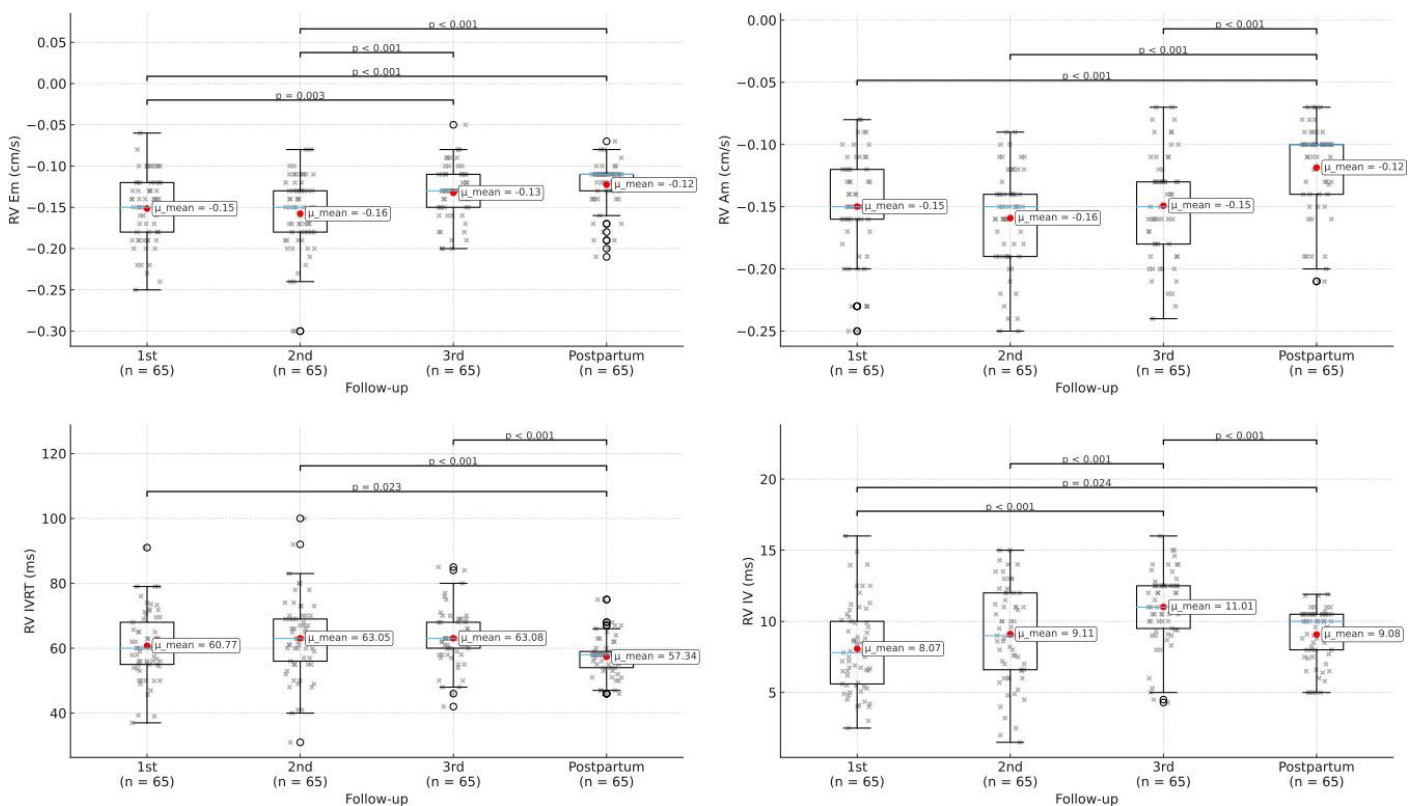


**Figure 5. Longitudinal changes in tissue Doppler imaging-derived (TDI-derived) right ventricular (RV) diastolic parameters across pregnancy and postpartum. Changes in RV diastolic function assessed by TDI, including early diastolic myocardial velocity (RV Em), atrial contraction velocity (RV Am), RV lateral isovolumetric relaxation time (IVRT), and RV lateral isovolumetric velocity (IVV).**

which is consistent with prior reports indicating that subtle systolic adjustments may accompany gestational remodeling. In parallel, left atrial area and deceleration time increased during pregnancy, supporting the presence of volume-related adaptive changes consistent with established physiological expectations.

Importantly, our findings demonstrate that several deformation-based diastolic and atrial indices did not fully return to first-trimester values in the early postpartum period. Rather than implying pathology, these observations indicate that mechanical recovery is heterogeneous and may extend beyond the traditional

**Table 3. Changes in strain–rate parameters during pregnancy and the postpartum period**

Strain rate parameters	1 <sup>st</sup> trimester	2 <sup>nd</sup> trimester	3 <sup>rd</sup> trimester	Postpartum	P
Basal and apical circumferential/radial strain–rate components					
Baz SR S (s <sup>-1</sup> )	-1.35 ± 0.35	-1.31 ± 0.25	-1.20 ± 0.23	-1.13 ± 0.29	<0.001 <sup>b,c,e</sup>
Baz SR E (s <sup>-1</sup> )	1.44 ± 0.44	1.34 ± 0.36	1.30 ± 0.56	1.37 ± 0.31	0.299
Baz SR A (s <sup>-1</sup> )	0.674 ± 0.33	0.635 ± 0.33	0.727 ± 0.34	0.678 ± 0.28	0.441
Baz RSR S (s <sup>-1</sup> )	1.72 ± 0.55	1.74 ± 0.37	1.62 ± 0.40	1.74 ± 0.37	0.319
Baz RSR E (s <sup>-1</sup> )	-1.88 ± 0.73	-1.72 ± 0.66	-1.46 ± 0.63	-1.58 ± 0.53	0.002 <sup>b,c</sup>
Baz RSR A (s <sup>-1</sup> )	-1.11 ± 0.46	-1.22 ± 0.63	-1.41 ± 0.66	-0.97 ± 0.36	<0.001 <sup>b,f</sup>
Ap CSR S (s <sup>-1</sup> )	-1.97 ± 0.78	-1.74 ± 0.51	-1.96 ± 0.74	-1.80 ± 0.32	0.085
Ap CSR E (s <sup>-1</sup> )	<b>2.56 ± 1.02</b>	<b>1.96 ± 0.82</b>	<b>1.76 ± 1.03</b>	<b>1.91 ± 0.71</b>	<b>&lt;0.001<sup>a,b,c</sup></b>
Ap CSR A (s <sup>-1</sup> )	0.914 ± 0.59	0.972 ± 0.69	1.22 ± 0.63	0.908 ± 0.56	0.015 <sup>b,f</sup>
Ap RSR S (s <sup>-1</sup> )	1.39 ± 0.65	1.47 ± 0.60	1.60 ± 0.69	1.70 ± 0.52	0.026 <sup>e</sup>
Ap RSR E (s <sup>-1</sup> )	-1.93 ± 0.87	-1.82 ± 0.89	-1.83 ± 0.91	-1.72 ± 0.77	0.587
Ap RSR A (s <sup>-1</sup> )	-0.864 ± 0.58	-0.995 ± 0.71	-1.45 ± 0.93	-1.34 ± 0.54	<0.001 <sup>b,c,d,e</sup>
Longitudinal strain rate components (2C/3C/4C)					
LSR S 4c (s <sup>-1</sup> )	-1.18 ± 0.17	-1.15 ± 0.19	-1.14 ± 0.16	-1.10 ± 0.12	0.041 <sup>e</sup>
LSR E 4c (s <sup>-1</sup> )	<b>1.59 ± 0.26</b>	<b>1.56 ± 0.26</b>	<b>1.31 ± 0.37</b>	<b>1.29 ± 0.34</b>	<b>&lt;0.001<sup>b,c,d,e</sup></b>
LSR A 4c (s <sup>-1</sup> )	0.826 ± 0.24	0.782 ± 0.18	0.772 ± 0.26	0.784 ± 0.11	0.479
LSR S 2c (s <sup>-1</sup> )	-1.19 ± 0.22	-1.22 ± 0.20	-1.23 ± 0.22	-1.19 ± 0.16	0.553
LSR E 2c (s <sup>-1</sup> )	<b>1.57 ± 0.42</b>	<b>1.53 ± 0.41</b>	<b>1.32 ± 0.34</b>	<b>1.36 ± 0.29</b>	<b>&lt;0.001<sup>b,c,d,e</sup></b>
LSR A 2c (s <sup>-1</sup> )	0.819 ± 0.24	0.861 ± 0.23	0.954 ± 0.27	0.878 ± 0.21	0.014 <sup>b</sup>
LSR S 3c (s <sup>-1</sup> )	-1.16 ± 0.19	-1.15 ± 0.22	-1.13 ± 0.18	-1.01 ± 0.29	<0.001 <sup>c, e, f</sup>
LSR E 3c (s <sup>-1</sup> )	<b>1.61 ± 0.36</b>	<b>1.45 ± 0.34</b>	<b>1.31 ± 0.39</b>	<b>1.09 ± 0.33</b>	<b>&lt;0.001<sup>b,c,e,f</sup></b>
LSR A 3c (s <sup>-1</sup> )	0.847 ± 0.25	0.704 ± 0.19	0.820 ± 0.28	0.711 ± 0.22	<0.001 <sup>a,c,d,f</sup>
LA and RA strain rate					
LA SR S (s <sup>-1</sup> )	1.84 ± 0.50	1.76 ± 0.43	1.82 ± 0.65	1.81 ± 0.44	0.833
LA SR E (s <sup>-1</sup> )	<b>-2.26 ± 0.65</b>	<b>-1.85 ± 0.51</b>	<b>-1.82 ± 0.64</b>	<b>-2.25 ± 0.65</b>	<b>&lt;0.001<sup>a,b,e,f</sup></b>
LA SR A (s <sup>-1</sup> )	<b>-1.89 ± 0.78</b>	<b>-1.55 ± 0.56</b>	<b>-1.89 ± 0.87</b>	<b>-1.77 ± 0.60</b>	<b>0.020<sup>a,d</sup></b>
RA SR S (s <sup>-1</sup> )	1.85 ± 0.53	1.74 ± 0.46	2.06 ± 0.85	2.19 ± 0.48	<0.001 <sup>c, d, e</sup>
RA SR E (s <sup>-1</sup> )	<b>-1.92 ± 0.75</b>	<b>-1.51 ± 0.53</b>	<b>-2.13 ± 1.05</b>	<b>-1.42 ± 0.77</b>	<b>&lt;0.001<sup>a,c,d,e</sup></b>
RA SR A (s <sup>-1</sup> )	<b>-1.62 ± 0.61</b>	<b>-1.39 ± 0.52</b>	<b>-1.57 ± 0.72</b>	<b>-1.36 ± 0.54</b>	<b>0.04<sup>e</sup></b>

Ap CSR S/E/A, Apical circumferential strain rate (systolic, early diastolic, late diastolic); Ap RSR S/E/A, Apical radial strain rate (systolic, early diastolic, late diastolic); Baz RSR S/E/A, Basal radial strain rate (systolic, early diastolic, late diastolic); Baz SR S/E/A, Basal segment strain rate (systolic, early diastolic, late diastolic). LSR S/E/A 4c, Longitudinal strain rate in the four–chamber view (systolic, early diastolic, late diastolic); LSR S/E/A 2c, Longitudinal strain rate in the two–chamber view; LSR S/E/A 3c, Longitudinal strain rate in the three–chamber view. LA SR S/E/A, Left atrial strain rate (systolic, early diastolic, late diastolic); RA SR S/E/A, Right atrial strain rate (systolic, early diastolic, late diastolic). a, First trimester vs. second trimester; b, First trimester vs. third trimester; c, First trimester vs. postpartum; d, Second trimester vs. third trimester; e, Second trimester vs. postpartum; f, Third trimester vs. postpartum.

6–12–week interval. This aligns with recent insights highlighted in the 2025 ESC Guidelines, which describe the postpartum period as a vulnerable stage of cardiovascular adaptation,<sup>3</sup> and our results contribute complementary evidence by showing that even in healthy pregnancies, normalization of myocardial mechanics may follow a more protracted trajectory.

**Ongoing Remodeling in the Early Postpartum Period**

A notable finding of our study was that several diastolic indices did not return to first–trimester levels in the early postpartum period. Both early diastolic strain rate and lateral Em velocity remained lower than baseline, suggesting that normalization of myocardial

relaxation may extend beyond the standard 6–12–week window. Although E/Em ratios (lateral, septal, and averaged) were mildly elevated compared with first–trimester measurements, all values remained within normal physiological limits, supporting the interpretation that these differences most likely reflect residual physiological adaptation rather than increased filling pressures.

These observations align with prior studies demonstrating that diastolic adjustment often continues into the postpartum period, even in uncomplicated pregnancies.<sup>9,17</sup> The pattern of delayed normalization observed in our cohort also mirrors trends described in hypertensive pregnancies. For instance, Muthyala

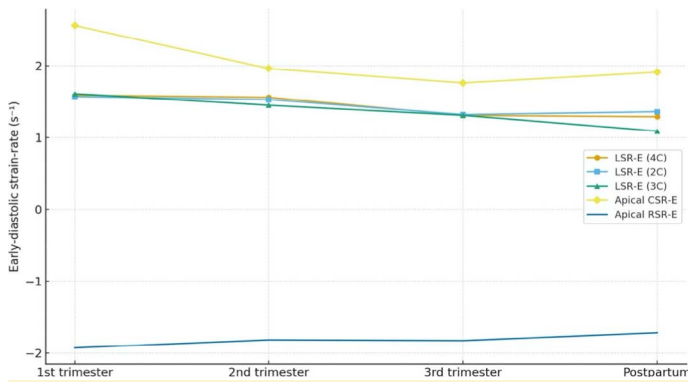


**Figure 6. Early-diastolic strain-rate parameters across pregnancy and early postpartum.** Line plots showing trimester-specific and postpartum changes in early diastolic strain-rate indices, including longitudinal strain rate during early diastole (LSR-E) from 4C, 2C, and 3C views, apical circumferential strain rate during early diastole (CSR-E), and apical radial strain rate during early diastole (RSR-E). Values represent mean ± standard deviation (SD).

et al.<sup>18</sup> in 2016 reported persistent diastolic abnormalities in a proportion of women with preeclampsia, proportional to disease severity. While our population consisted exclusively of normotensive women, the similarity in temporal recovery patterns suggests that postpartum diastolic remodeling may represent a continuum of physiological adaptation rather than a pathological extension of hypertensive pregnancy mechanisms.

Taken together, these findings indicate that cardiac recovery after pregnancy may be more gradual than traditionally assumed, supporting calls to re-examine the temporal boundaries of the “physiological” postpartum period.<sup>4,5</sup> Even among healthy women, subtle deviations from baseline mechanics may persist transiently, underscoring the value of sensitive imaging parameters in characterizing postpartum cardiovascular adaptation.

**Rotational Mechanics and Energy Adaptation in the Postpartum Heart**

Rotational mechanics findings in our cohort provide additional context for myocardial adaptation after delivery. We observed a postpartum decrease in apical rotation and global LV twist, suggesting an attenuation of the torsional augmentation that characterizes late gestation. This pattern differs from the increased twist reported by Ari et al.<sup>19</sup> in 2020 in late pregnancy, likely reflecting methodological differences in timing and population characteristics.

In our study, the reduction in twist was accompanied by a modest decline in LVEF and a significant decrease in apical early diastolic rotational rate (Ap RR-E). While these findings may indicate a physiological adjustment as hemodynamic load decreases after delivery, the underlying mechanisms cannot be fully determined from imaging data alone. Therefore, rather than implying intrinsic changes in fiber orientation or energetics, our results more conservatively suggest a postpartum recalibration of torsional dynamics that parallels the observed changes in diastolic function.

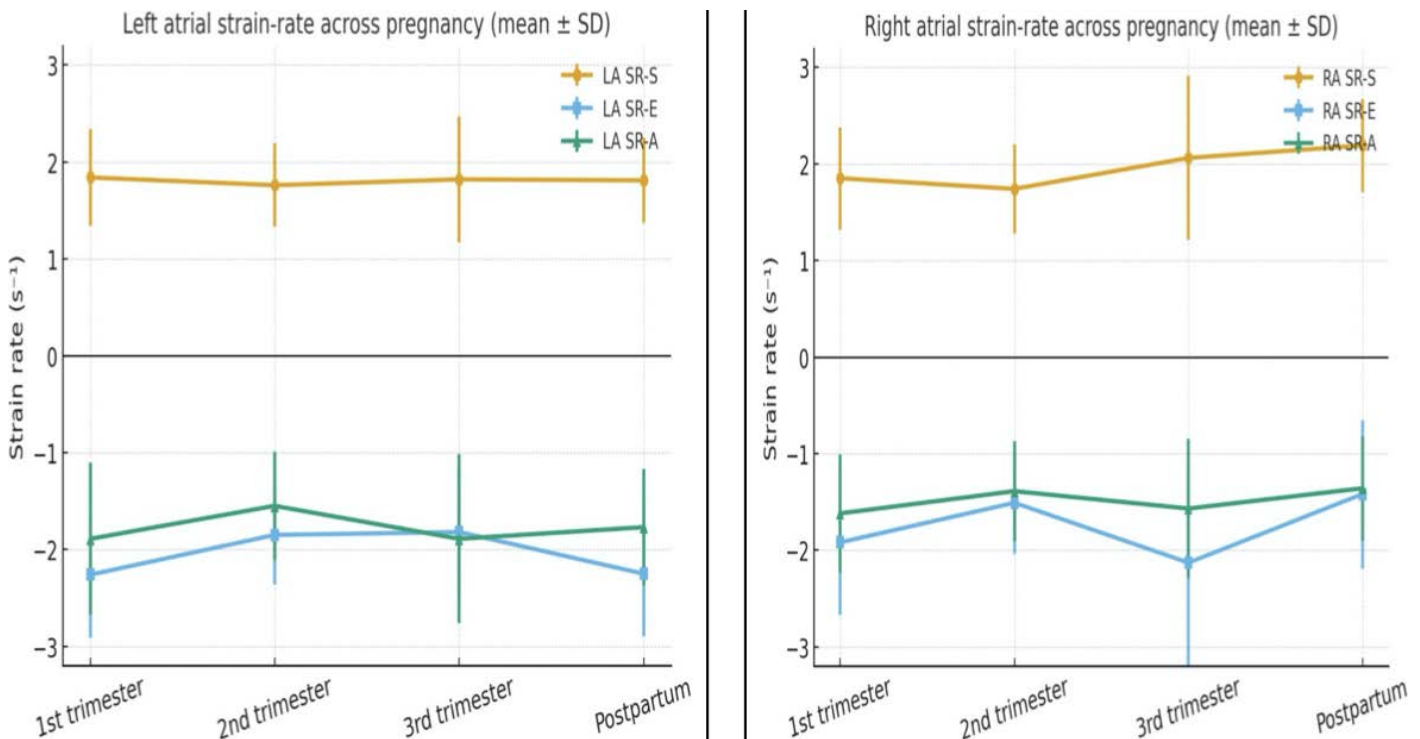


**Figure 7. Left and right atrial strain-rate parameters (SR-S, SR-E, SR-A) across pregnancy and postpartum.** Grouped line-plots demonstrating temporal changes in atrial systolic strain rate (SR-S), early diastolic strain rate (SR-E), and late diastolic strain rate (SR-A) for the left atrium (left panel) and right atrium (right panel). All values are shown as mean ± standard deviation (SD).

Because our postpartum follow-up was limited to 6–12 weeks, it remains unclear whether these torsional alterations fully normalize with longer recovery. Future studies with extended postpartum surveillance and integration of clinical, metabolic, and myocardial energetic markers will be essential to clarify whether reduced twist represents a transient physiological adaptation or has implications for long-term remodeling.

### **Biatrial Functional Adaptation Across Pregnancy and Postpartum**

Our study is among the few to longitudinally evaluate both left and right atrial mechanics during pregnancy using strain-rate imaging. We identified trimester-related changes in LA and RA strain-rate parameters, with only partial normalization in the early postpartum period. These findings are consistent with Guler et al.<sup>20</sup> in 2024, who reported progressive increases in right atrial reservoir and contraction strain during gestation and incomplete normalization after delivery. Similarly, Song et al.<sup>21</sup> in 2015 and Tasar et al.<sup>22</sup> in 2019 documented declines in left atrial reservoir and conduit strain during pregnancy and variable recovery trajectories postpartum, with conduit function showing slower improvement. Our observations parallel these reports, demonstrating reductions in LA SR-E and SR-A during pregnancy and incomplete restoration by 6–12 weeks postpartum.

It is important to recognize that atrial reservoir and conduit strain are influenced by dynamic loading conditions, including LV base descent and end-diastolic volumes. Because full hemodynamic normalization may not occur until 3–6 months after delivery, modest deviations from baseline in our early postpartum measurements likely reflect the expected physiological recovery timeline rather than persistent dysfunction. Nonetheless, the persistence of altered atrial strain-rate indices despite improvement in preload-sensitive parameters suggests that atrial adaptation may involve intrinsic, chamber-specific remodeling processes.

These findings support the potential value of incorporating biatrial deformation indices into peripartum echocardiographic protocols to enhance phenotypic characterization and improve understanding of maternal cardiovascular adaptation.

Moreover, given that hemodynamic loading conditions during labor differ between vaginal and cesarean delivery, the mode of delivery may theoretically influence the trajectory of postpartum myocardial recovery. Although our study population was not large enough to permit adequately powered subgroup analyses, understanding whether ventricular or atrial deformation indices normalize differently according to delivery mode is an important avenue for future investigation. Larger cohorts may help clarify whether labor-related hemodynamic stress modifies early postpartum myocardial mechanics, potentially contributing to more individualized postpartum surveillance strategies.

### **Diagnostic Sensitivity of Advanced Echocardiographic Techniques**

In our cohort, the application of strain rate imaging—characterized by superior temporal resolution and reduced preload dependency—appeared particularly valuable. Even with preserved LVEF, significant alterations in strain rate and rotational mechanics were detectable, underscoring the ability of advanced imaging to reveal subclinical myocardial changes

that may remain concealed with conventional indices. These observations are in agreement with prior reports<sup>12,23</sup> and suggest that broader integration of deformation imaging into peripartum assessment protocols could improve the sensitivity of cardiovascular evaluation in pregnancy. While the prognostic implications of such findings require further study, our results support the potential of advanced echocardiographic modalities to complement standard measures in monitoring maternal cardiac adaptation.

### **Study Contributions and Methodological Considerations**

This study offers several methodological contributions. First, it is among the few longitudinal investigations to apply strain rate imaging across all trimesters and into the postpartum period, thereby detecting subtle myocardial alterations not captured by conventional Doppler indices. Second, the systematic evaluation of biatrial function provided chamber-specific insights that are often overlooked in pregnancy-related cardiovascular research. Third, the demonstration of reduced postpartum twist despite preserved systolic function introduces the concept of transient physiological energy redistribution following delivery.

Collectively, these findings question the assumption that cardiovascular recovery is universally complete within 6–12 weeks postpartum. While the prognostic implications remain to be established, they suggest that extended monitoring may be warranted even in otherwise healthy pregnancies and highlight the value of advanced imaging for refining our understanding of maternal cardiac adaptation.

### **Limitations**

Several limitations of this study should be acknowledged. First, it was conducted at a single center in a relatively homogenous cohort of healthy, low-risk pregnant women. As such, the findings may not be fully generalizable to more heterogeneous populations, including high-risk pregnancies, women with comorbid conditions, or those of advanced maternal age. Given that cardiovascular adaptation to pregnancy can vary substantially across clinical scenarios, selection bias cannot be excluded.

Second, the advanced echocardiographic parameters applied—particularly strain rate and rotational mechanics—are inherently operator dependent. Although all measurements were performed by a single experienced observer and intra-observer reproducibility was excellent (ICC > 0.85), variability related to equipment, analysis software, or operator expertise may limit the broader applicability of the protocol.

Third, postpartum assessment was confined to the early recovery phase (6–12 weeks). Our observations suggest that recovery may extend beyond this interval; therefore, studies incorporating longer follow-up, ideally beyond six months, are warranted to define the complete timeline of postpartum cardiac normalization.

Fourth, the study focused primarily on physiological adaptation mechanisms and did not include complementary measures such as biomarkers (e.g., N-terminal pro-B-type natriuretic peptide [NT-proBNP], troponin, oxidative stress markers) or clinical symptom scores. The absence of these correlates limits interpretation of the clinical and prognostic significance of the echocardiographic findings.

Finally, certain structural and hemodynamic variables—including left ventricular mass index, indexed atrial volumes, right ventricular volumes, and pulmonary artery pressures—were not assessed. Incorporating these measures might have provided a more comprehensive picture of global cardiac remodeling.

Despite these limitations, this prospective longitudinal study provides valuable insights by applying advanced echocardiographic modalities to characterize time-sensitive maternal cardiac adaptation. The findings suggest that even in low-risk pregnancies, postpartum recovery may be more protracted than traditionally assumed, and that deformation imaging can sensitively detect these subtle physiological transitions.

### Conclusion

This prospective longitudinal study provides novel insights into maternal cardiac adaptation by applying advanced echocardiographic techniques across pregnancy and into the postpartum period. Despite preserved ejection fraction, subclinical alterations in strain rate, atrial function, and rotational mechanics were detected, underscoring the added diagnostic value of deformation imaging beyond conventional parameters.

The incomplete normalization of diastolic and torsional indices in the early postpartum phase suggests that cardiovascular recovery may extend beyond the traditionally accepted 6-12-week interval. These observations indicate that even in healthy pregnancies, recovery may be gradual and heterogeneous across individuals.

The 2025 ESC Guidelines on the management of cardiovascular disease and pregnancy define pregnancy as a natural cardiovascular stress test and a critical window into women's future heart health.<sup>3</sup> Our findings are consistent with this perspective and suggest that advanced imaging modalities may support more sensitive postpartum surveillance strategies. Such an approach could enable earlier recognition of subclinical myocardial changes and, ultimately, contribute to preventive strategies aimed at preserving long-term maternal cardiovascular health.

**Ethics Committee Approval:** Ethics committee approval was obtained from Kartal Koşuyolu High Specialization Training and Research Hospital Scientific Research Ethics Committee (Approval Number: 2025/12/1196, Date: 22.07.2025).

**Informed Consent:** Written informed consent was obtained from all participants.

**Conflict of Interest:** The authors have no conflicts of interest to declare.

**Funding:** The authors declared that this study received no financial support.

**Use of AI for Writing Assistance:** The authors declare that no artificial intelligence (AI)-assisted technologies were used in the writing or editing of the manuscript, nor in the creation of figures, tables, or illustrations.

**Author Contributions:** Concept – S.T.U., A.K.; Design – A.K.; Supervision – R.D.A.; Resource – B.Keskin, M.K.; Materials – M.K.; Data Collection and/or Processing – B.Keskin, A.K.; Analysis and/or Interpretation – B.Kültürsay; Literature Review – S.T.U.; Writing – S.T.U.; Critical Review – A.K.

**Peer-review:** Externally peer-reviewed.

### References

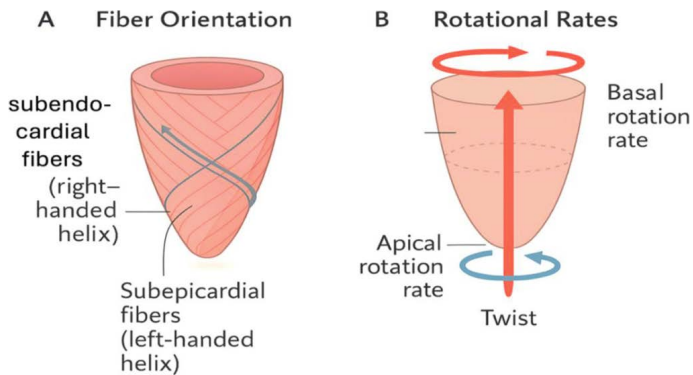
1. Meah VL, Cockcroft JR, Backx K, Shave R, Stöhr EJ. Cardiac output and related haemodynamics during pregnancy: a series of meta-analyses. *Heart*. 2016;102(7):518-526. [CrossRef]
2. Sanghavi M, Rutherford JD. Cardiovascular physiology of pregnancy. *Circulation*. 2014;130(12):1003-1008. [CrossRef]
3. De Backer J, Haugaa KH, Hasselberg NE, et al.; ESC Scientific Document Group. 2025 ESC Guidelines for the management of cardiovascular disease and pregnancy. *Eur Heart J*. 2025;46(43):4462-4568. Erratum in: *Eur Heart J*. 2025;ehaf1011. [CrossRef]
4. Melchiorre K, Sharma R, Khalil A, Thilaganathan B. Maternal Cardiovascular Function in Normal Pregnancy: Evidence of Maladaptation to Chronic Volume Overload. *Hypertension*. 2016;67(4):754-762. [CrossRef]
5. Mehta LS, Warnes CA, Bradley E, et al.; American Heart Association Council on Clinical Cardiology; Council on Arteriosclerosis, Thrombosis and Vascular Biology; Council on Cardiovascular and Stroke Nursing; and Stroke Council. Cardiovascular Considerations in Caring for Pregnant Patients: A Scientific Statement from the American Heart Association. *Circulation*. 2020;141(23):e884-e903. Erratum in: *Circulation*. 2021;143(12):e792-e793. [CrossRef]
6. Kayıkçoğlu M, Biteker M, Mutluer FO, et al.; Artemis Investigators. Baseline Characteristics and Clinical Insights from the ARTEMIS Registry: A Comprehensive Study of Peripartum Cardiomyopathy in Türkiye. *Turk Kardiyol Dern Ars*. 2024;52(7):474-483. [CrossRef]
7. Taçoy G, Karçaaltıncaba D, Türkoğlu S. Cardiovascular Diseases During Pregnancy. *Turk Kardiyol Dern Ars*. 2024;52(7):536-540. [CrossRef]
8. Fok WY, Chan LY, Wong JT, Yu CM, Lau TK. Left ventricular diastolic function during normal pregnancy: assessment by spectral tissue Doppler imaging. *Ultrasound Obstet Gynecol*. 2006;28(6):789-793. [CrossRef]
9. Bamfo JE, Kametas NA, Nicolaidis KH, Chambers JB. Maternal left ventricular diastolic and systolic long-axis function during normal pregnancy. *Eur J Echocardiogr*. 2007;8(5):360-368. [CrossRef]
10. Hieda M, Yoo JK, Sun DD, et al. Time course of changes in maternal left ventricular function during subsequent pregnancy in women with a history of gestational hypertensive disorders. *Am J Physiol Regul Integr Comp Physiol*. 2018;315(4):R587-R594. [CrossRef]
11. Jasaityte R, D'Hooge J. Strain rate imaging: Fundamental principles and progress so far. *Imaging in Med*. 2010;2(5):547-563. [CrossRef]
12. Voigt JU, Pedrizzetti G, Lysyansky P, et al. Definitions for a common standard for 2D speckle tracking echocardiography: consensus document of the EACVI/ASE/Industry Task Force to standardize deformation imaging. *Eur Heart J Cardiovasc Imaging*. 2015;16(1):1-11. [CrossRef]
13. Naqvi TZ, Meena Narayanan, Rafie R, et al. Cardiovascular Adaptation in Normal Pregnancy With 2D and 3D Echocardiography, Speckle Tracking, and Radial Artery Tonometry. *JACC Adv*. 2024;3(11):101360. [CrossRef]
14. Lang RM, Badano LP, Mor-Avi V, et al. Recommendations for cardiac chamber quantification by echocardiography in adults: an update from the American Society of Echocardiography and the European Association of Cardiovascular Imaging. *Eur Heart J Cardiovasc Imaging*. 2015;16(3):233-270. Erratum in: *Eur Heart J Cardiovasc Imaging*. 2016;17(4):412. Erratum in: *Eur Heart J Cardiovasc Imaging*. 2016;17(9):969. [CrossRef]
15. Nagueh SF, Smiseth OA, Appleton CP, et al. Recommendations for the Evaluation of Left Ventricular Diastolic Function by Echocardiography: An Update from the American Society of Echocardiography and the European Association of Cardiovascular Imaging. *J Am Soc Echocardiogr*. 2016;29(4):277-314. [CrossRef]
16. Sade LE, Joshi SS, Cameli M, Cosyns B, et al. Current clinical use of speckle-tracking strain imaging: insights from a worldwide survey from the European Association of Cardiovascular Imaging (EACVI). *Eur Heart J Cardiovasc Imaging*. 2023;24(12):1583-1592. [CrossRef]

17. Meah VL, Backx K, Cockcroft JR, Shave RE, Stöhr EJ. Left ventricular mechanics in late second trimester of healthy pregnancy. *Ultrasound Obstet Gynecol.* 2019;54(3):350-358. [\[CrossRef\]](#)
18. Muthyala T, Mehrotra S, Sikka P, Suri V. Maternal Cardiac Diastolic Dysfunction by Doppler Echocardiography in Women with Preeclampsia. *J Clin Diagn Res.* 2016;10(8):QC01- QC03. [\[CrossRef\]](#)
19. Ari S, Ari H, Yılmaz M, Bozat T. Evaluation of myocardial function in pregnant women with speckle-tracking echocardiography. *Eur Res J.* 2020;6(6):615-623. [\[CrossRef\]](#)
20. Guler Y, Karagoz A, Inan D, et al. Quantitative Analysis of Right Atrial Functions by 2D-Speckle Tracking Echocardiography During Healthy Pregnancy. *J Ultrasound Med.* 2024;43(11):2087-2093. [\[CrossRef\]](#)
21. Song G, Liu J, Ren W, et al. Reversible Changes of Left Atrial Function during Pregnancy Assessed by Two-Dimensional Speckle Tracking Echocardiography. *PLoS One.* 2015;10(5):e0125347. [\[CrossRef\]](#)
22. Tasar O, Kocabay G, Karagoz A, et al. Evaluation of Left Atrial Functions by 2-dimensional Speckle-Tracking Echocardiography During Healthy Pregnancy. *J Ultrasound Med.* 2019;38(11):2981-2988. [\[CrossRef\]](#)
23. Paudel A, Tigen K, Yoldemir T, et al. The evaluation of ventricular functions by speckle tracking echocardiography in preeclamptic patients. *Int J Cardiovasc Imaging.* 2020;36(9):1689-1694. [\[CrossRef\]](#)

**Appendix Table 1. Atrial reservoir and conduit strain across pregnancy and the postpartum period**

Parameter	1 <sup>st</sup> trimester	2 <sup>nd</sup> trimester	3 <sup>rd</sup> trimester	Postpartum	P
LA reservoir strain (%)	39.77 ± 11.04	33.00 ± 9.15	34.85 ± 12.71	42.08 ± 9.94	<0.001
LA conduit strain (%)	16.02 ± 7.47	12.46 ± 6.28	13.95 ± 7.61	16.12 ± 6.82	<0.001
RA reservoir strain (%)	32.40 ± 10.81	27.68 ± 7.52	30.65 ± 11.82	38.75 ± 6.86	<0.001
RA conduit strain (%)	15.17 ± 6.51	12.48 ± 5.13	14.43 ± 5.69	16.41 ± 3.74	<0.001

LA, Left atrium; RA, Right atrium.



**Appendix Figure 1. Schematic representation of left ventricular rotational mechanics. Conceptual diagram illustrating the underlying principles of left ventricular (LV) twisting mechanics. Panel A shows opposing subendocardial (right-handed helix) and subepicardial (left-handed helix) fiber orientations. Panel B depicts basal clockwise rotation, apical counterclockwise rotation, and the resulting net LV twist.**